

This is the accepted manuscript version of the contribution published as:

Romano, P., Simonetti, S., Gambi, M.C., **Luckenbach, T.**, Zupo, V., Corsi, I. (2024):
Preliminary investigation on the potential involvement of an ABC-like gene in
Halomicronema metazoicum (Cyanobacteria) tolerance to low seawater pH in an ocean
acidification scenario
Mar. Pollut. Bull. **205** , art. 116584

The publisher's version is available at:

<https://doi.org/10.1016/j.marpolbul.2024.116584>

1 **Preliminary investigation on the potential involvement of an ABC-like gene in *Halomiconema***
2 ***metazoicum* (Cyanobacteria) tolerance to low seawater pH in an ocean acidification scenario**

3

4 Patrizia Romano ^{a, b, 1, *}, Silvia Simonetti ^{a, c, 1, *}, Maria Cristina Gambi ^d, Till Luckenbach ^e, Valerio Zupo ^c,
5 Ilaria Corsi ^a

6

7 ^a Department of Physical, Earth and Environmental Sciences, University of Siena, via Mattioli, 4, 53100 Siena,
8 Italy

9 ^b Stazione Zoologica Anton Dohrn, National Institute of Marine Biology, Ecology and Biotechnology,
10 Department of BEOM, Napoli, Italy

11 ^c Stazione Zoologica Anton Dohrn, National Institute of Marine Biology, Ecology and Biotechnology,
12 Integrative Marine Ecology Department, Napoli, Italy

13 ^d National Institute of Oceanography and Applied Geophysics, OGS, Trieste, Italy

14 ^e Department Ecotoxicology, Helmholtz Centre for Environmental Research (UFZ), Leipzig, Germany

15

16 ¹ These authors have equally contributed to the work.

17

18 * Corresponding authors at: Department of Physical, Earth and Environmental Sciences, University of Siena,
19 via Mattioli, 4, 53100 Siena (Italy); E-mail addresses: silvia.simonetti@student.unisi.it (S. Simonetti) and
20 patrizia.romano@student.unisi.it (P. Romano)

21 **Abstract**

22 Decreasing ocean surface pH, called ocean acidification (OA), is among the major risks for marine ecosystems
23 due to human-driven atmospheric $p\text{CO}_2$ increase. Understanding the molecular mechanisms of adaptation
24 enabling marine species to tolerate a lowered seawater pH could support predictions of consequences of future
25 OA scenarios for marine life. This study examined whether the ATP-binding cassette (ABC)-like gene *slr2019*
26 confers tolerance to the marine cyanobacterium *Halomicronema metazoicum* to low seawater pH conditions
27 (7.7, 7.2, 6.5) in short- and long-term exposures (7 and 30 d). Photosynthetic pigment content indicated that
28 the species can tolerate all three lowered-pH conditions. At day 7, *slr2019* was up-regulated at pH 7.7 while
29 no changes were observed at lower pH. After 30-d exposure, a significant decrease in *slr2019* transcript levels
30 was observed in all low-pH treatments. These first results indicate an effect of low pH on the examined
31 transporter expression in *H. metazoicum*.

32

33 **Keywords:** *Halomicronema metazoicum*, Cyanobacteria, acid stress tolerance, ATP-binding cassette (ABC)
34 membrane transporter proteins, ocean acidification (OA) scenarios, low pH

35 1. Introduction

36 Since the beginning of the industrial revolution, the mean surface pH of oceans dropped from approximately
37 8.2 to 8.1 due to past and current carbon dioxide (CO₂) emissions (Jiang et al., 2019), and the trend is expected
38 to continue until the end of the century (estimated further decrease by up to 0.4 pH units by the year 2100)
39 (Bindoff et al., 2019). The resulting ocean acidification (OA) represents a significant environmental threat to
40 marine life (Alter et al., 2024; Doney et al., 2009). Relevant studies aimed at predicting the effects of future
41 OA scenarios on coastal ecosystems have been carried out in naturally acidified areas (e.g. CO₂ vents),
42 revealing several impacts from reductions in habitat complexity and species richness (Kroeker et al., 2013;
43 Gambi et al., 2016; Muralisankar et al., 2021; Fanelli et al., 2022; Munari et al., 2022; Xie et al., 2023), to
44 simplification of food webs and reduction of ecosystem functions (Vizzini et al., 2017; Teixidó et al., 2018).
45 However, certain species exhibit remarkable abilities to tolerate natural low-pH/high-pCO₂ conditions (Gambi
46 et al., 2016). Such adapted organisms can provide important insights into cellular and molecular mechanisms
47 allowing marine species to cope with acidified environments.

48 Molecular responses affecting the cell integrity of marine species towards exposure to low pH have been
49 examined but the cellular mechanisms driving tolerance remain to a large extent unclear (reviewed in Simonetti
50 et al., 2022). Findings on prokaryotes dealing with highly acidified environments suggest the involvement of
51 ATP-binding cassette (ABC) transport proteins in conferring resistance to acidic conditions by a relocation of
52 endogenous substances, such as ATP, carbohydrates and lipids, that contribute to maintaining intracellular
53 homeostasis (Zhu et al., 2019). This was found in cyanobacteria (*Synechocystis* sp. and *Anabaena* sp.; pH from
54 3.0 to 6.0) (Tahara et al., 2012; 2015; Matsushashi et al., 2015; Uchiyama et al., 2019; Shvarev and Maldene,
55 2020), human gastric microbiota (*Helicobacter pylori*) (McGowan et al., 1998) and bacteria in fermented foods
56 (*Acetobacter aceti*, *Acetobacter pasteurianus*, *Lactococcus lactis*) (Nakano et al., 2006; Gao et al., 2023, Zhu
57 et al., 2019).

58 In the present study, the ABC transporter-like gene *slr2019* of a free-living Cyanobacterium strain of
59 *Halomicronema metazoicum* was investigated for its potential role in conferring resistance to the impact of
60 acidified conditions. Slr2019 was selected as a candidate protein and it has been recognized as essential to
61 tolerate acid stress conditions in the cyanobacterium *Synechocystis* sp. PCC6803 (Matsushashi et al., 2015).
62 This work represents a first assessment of the involvement of ABC transporter proteins in *H. metazoicum*

63 resistance to low-pH/high- $p\text{CO}_2$ environments in order to clarify the general value of the hypothesis of the
64 essential role of these proteins in bacterial survival to acid stress. The species was selected as an
65 experimental model as it is known for its ability to cope with extreme environmental conditions, such as high
66 temperature, high salinity, and high irradiance (Mutalipassi et al., 2019a), and it is found to inhabit naturally
67 acidified marine areas (Ruocco et al., 2018). So far, there have been no investigations on an adaptive
68 mechanism behind the tolerance of the low natural pH conditions in the habitat of *H. metazoicum*. We here
69 present an experiment, in which cyanobacteria were exposed at pH conditions in the range from 0.4 to 1.6
70 units below the current natural seawater pH of 8.1, resembling potential future OA scenarios. Exposures
71 were for 7 and for 30 d and *slr2019* transcript levels were determined in parallel to cellular viability.
72 Since for *H. metazoicum* protocols for RNA extraction have not yet been established, different RNA extraction
73 methods were evaluated in this study.

74

75 **2. Materials and methods**

76 **2.1. *Halomicronema* culture conditions**

77 *Halomicronema metazoicum* mattes were obtained from permanent cultures maintained at the Stazione
78 Zoologica Anton Dohrn (Napoli, Italy), Ischia Marine Center at Villa Dohrn, Ischia and originating from leaves
79 of *Posidonia oceanica*, in a meadow off Lacco Ameno d'Ischia (Bay of Naples, 40°44'56" N, 13°53'13" E)
80 (Ruocco et al., 2018). Pure strains were grown in Guillard's *f/2* medium (Merck, Italy) and maintained under
81 sterile conditions in a thermostatic chamber at a temperature of 18 °C with light irradiance of about 200 μE
82 and a 12:12 light: dark photoperiod (see Mutalipassi et al., 2019b).

83 **2.2. Development of an RNA extraction method for *H. metazoicum***

84 The extraction of high yield and high-quality RNA from polysaccharide-rich matrices, such as those of a
85 filamentous cyanobacterium like *H. metazoicum*, poses specific challenges and no suitable RNA extraction
86 protocol has been established for the here studied cyanobacteria. We therefore designed and tested eight
87 different methods for RNA extraction from *H. metazoicum* cells (Figure 1A). Samples of approximately 100
88 mg fresh *H. metazoicum* mattes, stored in RNAlater (Sigma-Aldrich, USA) at -80 °C, were thawed, centrifuged

89 (4,500 rpm, 20 min, 4 °C) and the supernatant was removed. Prior to performing RNA isolation,
90 cyanobacterium cells were homogenized by high-intensity (HI) ultra-sonication (26 W, BANDELIN electronic
91 UW2070) as described by Kim Tiam et al. (2019), in order to successfully break up the cellular envelopes.
92 Samples in the extraction buffer were briefly vortexed and sonicated on ice four times for 30 s. After each
93 sonication, samples were vortexed. This homogenization step was used in all eight extraction methods.

94 **Method 1. Manual RNA extraction.** Samples were incubated in 1 ml TRIzol (Invitrogen, USA) extraction
95 buffer on ice for 30 min and then homogenized. After centrifugation (12,000 g, 5 min, 4 °C), 50 µL 1-Bromo-
96 3-Chloropropane (BCF) were added to the lower phase and re-centrifuged (12,000 g, 15 min, 4 °C). RNA was
97 precipitated by adding 0.5 vol RNA precipitation solution (1.2 M sodium chloride, 0.8 M sodium citrate) and
98 0.5 vol isopropyl alcohol to the upper phase and centrifuged (12,000 g, 15 min, 4 °C). The resulting pellet was
99 washed with 600 µL 75% ethanol, air dried and resuspended in 25 µL RNase-free water, followed by two
100 incubation steps, one of 15 min at 60 °C and one of 5 min at room temperature.

101 **Method 2. PureLink® RNA Mini Kit.** RNA from samples was isolated using the PureLink® RNA Mini Kit
102 (Ambion Life Technologies, USA) according to the manufacturer's protocol. Upon the procedure, RNA was
103 diluted in 40 µL RNase-free water.

104 **Method 3. TRIzol® reagent + PureLink® RNA Mini Kit.** In order to improve the lysis effectiveness, the
105 kit's lysis buffer was substituted with 1 mL TRIzol reagent. RNA isolation was performed following the 'Using
106 TRIzol® Reagent with the PureLink® RNA Mini Kit' method from the user guide. Extracted RNA was re-
107 suspended in a total volume of 40 µL RNase-free water.

108 **Method 4. Sample clarification with NaOH + PureLink® RNA Mini Kit.** An initial step with NaOH was
109 performed to dissolve extracellular substances, which could lower the extraction yield (Defrancesco et al.,
110 2002). Cyanobacterial mattes were incubated in 1 mL 1 M NaOH and centrifuged (4,500 rpm, 20 min, 4 °C).
111 Then RNA was extracted following the 'Using TRIzol® Reagent with the PureLink® RNA Mini Kit'
112 manufacturer's protocol.

113 **Method 5. NucleoSpin® RNA II Kit.** *H. metazoicum* mattes were incubated in 1 mL TRIzol reagent for 30
114 min on ice and homogenized. Then RNA was extracted by the NucleoSpin® RNA II kit (Macherey Nagel,
115 Germany), following the manufacturer's protocol. RNA was eluted in 40 µL RNase-free water.

116 **Method 6. NucleoSpin® miRNA Kit.** 50 mg of *H. metazoicum* mattes were used to extract RNA following
117 the NucleoSpin® miRNA Kit (Macherey Nagel, Germany) manufacturer's protocol. The purified RNA was
118 eluted in 30 µL RNase-free water.

119 **Method 7. TRIzol® reagent + NucleoSpin® miRNA Kit.** The Lysis Buffer ML of the NucleoSpin® miRNA
120 Kit was replaced with TRIzol reagent and then the manufacturer's protocol was followed. The isolated RNA
121 was eluted in 30 µL RNase-free water.

122 **Method 8. CTAB 2% buffer.** The RNA isolation method developed by Wang and Stegemann (2010) was
123 tested, with modification. Sixhundred µL pre-warmed (65 °C) 2% CTAB extraction buffer (200 mM Tris-HCl
124 (pH 8.00), 20 mM ethylenediaminetetraacetic acid, 1.4 M di sodium chloride, 1% polyvinylpyrrolidone 40)
125 were added to 100 mg of minced sample and vortexed for 5 min at room temperature. After the homogenization
126 step, an equal volume of chloroform:isoamyl alcohol (24:1) was mixed with the sample and centrifuged
127 (15,000 rcf, 5 min, room temperature). The clear upper phase was mixed again with an equal volume of
128 chloroform:isoamyl alcohol (24:1) and the centrifuge was repeated. Sixhundred µL isopropanol were added to
129 the upper phase and centrifuged (15,000 rcf, 15 min, room temperature). One mL 75% ethanol was added to
130 the lower phase and centrifuged (15,000 rcf, 15 min, room temperature). The pellet was dissolved in 50 µL
131 RNase-free water and purified following the manufacturer's protocol for the NucleoSpin® RNA II kit
132 (Macherey Nagel, Germany). Isolated RNA was diluted in 60 µL RNA-free water.

133 The quality of RNA obtained with the above-mentioned methods was assessed based on A_{260}/A_{280} and A_{260}/A_{230}
134 ratios measured on a BioPhotometer (Eppendorf 6131) and by electrophoresis on 1.5% agarose 'bleach gel'
135 (Aranda et al., 2012 modified) (visual inspection of 18S and 28S ribosomal RNA bands and for the lack of
136 visible genomic DNA contamination). The RNA concentration was quantified by absorbance at 260 nm on the
137 BioPhotometer.

138 **2.3. *In vivo* exposure of *H. metazoicum***

139 *Halomicronema metazoicum* mattes (approximately 1 g fresh weight) were isolated from the mother culture
140 and cultivated in sterile Guillard's *f/2* medium at pH 8.2, 7.7, 7.2, and 6.5, respectively, for 30 d in *ad hoc*
141 devised photobioreactors (more details in Mutalipassi et al., 2019b; Figure S1), under controlled temperature
142 and light conditions (18 °C, 12:12-h photoperiod). For each pH treatment, two photobioreactors were set up

143 (n = 2). Photobioreactors were composed of a Pyrex dish (2.4 L) covered with a heat-resistant glass plate
144 provided with a narrow hole in the middle. There, a pH probe (InLab Micro pH, Mettler Toledo) was housed
145 to constantly measure water pH. A pH controller (pH 201, Aqualight) was connected to the probe and to an
146 electronic valve regulating a centrifuge pump and a CO₂ regulator (CO₂ Energy, Ferplast) linked to the
147 photobioreactor through a glass pasteur pipette. The controller opened and closed the electronic valve, when
148 necessary, supplying CO₂ in order to regulate the pH. The centrifuge pump (Askoll Pure pump 300) was placed
149 inside the vessel and activated during CO₂ insufflation to avoid the formation of a pH gradient. Cyanobacterial
150 mattes were put in a perforated box located inside the dish. The water pH was checked three times per day to
151 ensure its stability (oscillations lower than 0.05 units). The chosen range of experimental pH values was
152 representative of present (pH 8.2) and potential future ocean pH scenarios (pH 7.7; predicted by Jiang et al.
153 (2019) for the end of the century in the scenario with CO₂ emissions remaining on the current high level). In
154 addition, one treatment was at pH 6.5 representing naturally acidified conditions occurring in the high CO₂
155 venting area at the Castello Aragonese, Ischia Island (Kroeker et al., 2011; Foo et al., 2018).
156 Mattes from each group were collected after 7 and 30 d and stored in RNA later (Sigma-Aldrich, USA) at -80
157 °C until analysis.

158 **2.4. Viability**

159 Viability of mattes was assessed qualitatively by observations of morphology and color of filaments according
160 to Ruocco et al. (2018) and by measuring chlorophyll *a* and carotenoid content according to the procedure of
161 Zavřel et al. (2015). Briefly, samples of 20 mg were centrifuged (15,000 *g*, 7 min, room temperature) and 1
162 mL 100% methanol (precooled at 4 °C) was added. The suspension was homogenized by vortexing, covered
163 with aluminum foil and incubated at 4 °C for 20 min to allow pigment extraction. After a second centrifugation
164 step (15,000 *g*, 7 min, 4 °C) the absorbance of the supernatant was measured by a spectrophotometer
165 (Shimadzu UV-VIS 160) at wavelengths 470, 665, and 720 nm against methanol as blank. The concentration
166 of pigments was calculated as:

$$167 \text{Chl}_a [\mu\text{g}/\text{mg}] = 12.9447 (A_{665} - A_{720}) / W$$

$$168 \text{Carotenoids} [\mu\text{g}/\text{mg}] = \{[1,000 (A_{470} - A_{720}) - 2.86 (\text{Chl}_a [\mu\text{g}/\text{mg}])] / 221\} / W$$

169 Where A_{470} , A_{665} , A_{720} were absorbance values measured at 470, 665 and 720 nm, respectively, and W was the
170 sample weight.

171 Pigments concentration was expressed as μg of pigments/mg of mattes.

172 2.5. ABC gene expression analysis

173 Two samples of 100 mg *H. metazoicum* cells were collected from each photobioreactor (4 replicates for each
174 pH treatments group) and RNA was extracted.

175 First-strand cDNA was synthesized from 175 ng of RNA (extracted with 'CTAB 2% buffer' method, method
176 8, see 3.1 below) in a final volume of 20 μL by using the qScript™ XLT cDNA SuperMix (Quantabio, USA)
177 according to the manufacturer's instructions (10 μL RNA template, 4 μL qScript XLT cDNA SuperMix (5X),
178 6 μL Rnase/Dnase-free water).

179 qPCR was performed in triplicate on an iCyclerIQ5 (Bio-Rad, USA) to amplify *slr2019* ABC-like transcript
180 (identified by Matsushashi et al., 2015) and *16S* (Ruocco et al., 2018) as a housekeeping gene. Each 20 μL
181 reaction contained 1 μL cDNA (diluted 10 times), 10 μL PerfeCTa® SYBR® Green SuperMix, Low ROX
182 (Quantabio, USA) and 1 μL of primer pairs. The thermal profile used was: an initial denaturation at 95 °C for
183 30 s, followed by 40 cycles of 5 s at 95 °C, 15 s at specific melting temperature for each primer pair (59 °C for
184 *16S* and 55 °C for *slr2019* gene), 10 s at 72 °C. The sequences of forward and reverse primers were 5'-
185 ACGGGGCGGCTGATG-3' and 5'-CAAAAATGCTCCACCAATCAC-3' for *slr2019* and 5'-
186 ATTGGGCGTAAAGCGTCCG-3' and 5'- TTCACCGTACTGGGAAT-3' for *16S* (see Table S1 for PCR
187 parameters). Relative quantification of gene expression levels was performed with the $2^{-\Delta\Delta\text{CT}}$ method (Livak
188 and Schmittgen, 2001).

189 The reaction efficiency was determined by a five-point dilution series through the equation: $E = (10^{(-1/\text{slope})} -$
190 $1) * 100$. The theoretical maximum of 100% indicates the doubling of the amount of product with each cycle.

191 2.6. Statistical analyses

192 The variance of pigment content and gene expression data was analyzed with the Kruskal-Wallis test, followed
193 by Dunn's multiple comparisons test. Differences were considered significant if $p < 0.05$. Statistical analyses

194 were performed using the software GraphPad Prism version 9.5.1 (528) for macOS (GraphPad Software,
195 USA).

196

197 **3. Results and discussion**

198 **3.1. RNA extraction methods**

199 The main obstacle to isolating pure, high-quality RNA from filamentous cyanobacteria is the mat's richness
200 in polysaccharides, which can affect both the yield and the quality of the extracted RNA. We thus tested
201 different protocols to isolate RNA from the filamentous cyanobacterium *H. metazoicum* to identify a method
202 yielding RNA of reasonable quality.

203 Yield (as ng of extracted RNA per mg of initial sample) and purity (assessed through A_{260}/A_{280} ratio and
204 A_{260}/A_{230} ratio) of RNA from each tested method are listed in Table 1; images of the bands of RNA isolates
205 upon agarose gel electrophoresis are in Figure 1B. The average A_{260}/A_{280} ratio and A_{260}/A_{230} ratio of the RNA
206 extracted from *H. metazoicum* varied from 1.57 to 2.13 and from 0.10 to 2.05, respectively, while the yield
207 was in the range of 1.13 ng_{RNA}/mg_{sample} and 14.88 ng_{RNA}/mg_{sample}. Only when using the 'CTAB 2% buffer'
208 method (method 8), pure, high-quality total RNA was obtained, with A_{260}/A_{280} and A_{260}/A_{230} ratios > 2 (highest
209 of all isolated) and the RNA yield among the highest (Table 1). The RNA isolate showed well-defined 28S
210 and 18S ribosomal RNA upon gel electrophoresis (Figure 1B). In contrast, the RNA isolated with all other
211 applied methods was less pure (A_{260}/A_{230} ratios of 0.1 - 1.52), resulting in more indistinct electrophoresis bands
212 (Figure 1B), and with a considerably lower yield in most cases (Table 1).

213 As suggested by Wang and Stegemann (2010), the 'CTAB 2% buffer' method seems to enable to obtain high-
214 quality RNA isolates by efficiently breaking up the filamentous envelope of the bacterial cells. The RNA
215 obtained with this method was suitable for qPCR analysis. The PCR efficiency resulted in 107% and 84% for
216 *16S*- and *slr2019*-primer pairs, respectively (Table S1), indicating the robustness of the method.

217 Based on these results, the 'CTAB 2% buffer' method was here applied for RNA extraction from all
218 experimental *H. metazoicum* samples.

219 **3.2. Viability**

220 *Halomicronema metazoicum* mattes of all four groups (three experimental groups and one control) were
221 characterized by macroscopic aggregates of filaments with a vivid emerald-green color until the end of the
222 experiment (Figure S2). According to our previous findings (Ruocco et al., 2018), the color of the *H.*
223 *metazoicum* mattes represents a suitable marker for the health status in its exponential phase of growth. Thus,
224 the color of the mattes indicates a good health status of the cyanobacteria incubated at different pH conditions.
225 Across all pH treatments and exposure durations, the chlorophyll *a* contents of cyanobacteria cells varied
226 between 0.13 (after 7 d exposure in mattes exposed to pH 7.7) and 0.31 $\mu\text{g}/\text{mg}$ (after 7 d exposure in mattes
227 exposed to pH 7.2). No significant differences were found in the chlorophyll *a* content of cells between control
228 and low pH groups, neither after 7 d nor after 30 d of exposure (Figure 2A). The chlorophyll *a* concentration
229 slightly increased between days 7 and 30 of exposure in control and pH-7.7 groups, while it was slightly lower
230 in the pH-7.2 and pH-6.5 groups, but the differences were not significant. After 7 d of exposure, chlorophyll
231 *a* slightly decreased in mattes exposed to pH 7.7 vs. controls while an increase in chlorophyll *a* was observed
232 in the pH-7.2 treatment. Mattes exposed to the most severe low pH of 6.5 had a chlorophyll *a* content similar
233 to the controls. After 30 d, no differences in chlorophyll *a* were found between the control and exposed groups
234 (Figure 2A).

235 The carotenoid amount was lower than chlorophyll *a* being in the range of 0.05, after 7 d at pH 7.7 and 0.12
236 $\mu\text{g}/\text{mg}$, after 7 d at pH 7.2, as previously observed in *H. metazoicum* samples from the Gulf of Taranto
237 (Northern Ionian Sea, Italy) (Caroppo et al., 2012). As for chlorophyll *a* content, the total carotenoids of
238 cyanobacteria cells were not significantly different between controls and any of the experimental low-pH
239 groups after 7 and 30 d of exposure (Figure 2B). The carotenoid concentrations in mattes derived from control
240 groups and from pH 7.7 and 6.5 exposures were slightly but not significantly higher after 30 d than after 7
241 exposure days. After 7 and 30 d of exposure, the carotenoid contents were slightly lower in the pH-7.7 group
242 and slightly higher in the pH-7.2 group than in the respective control groups ($p > 0.05$, no significance); in the
243 pH-6.5 group, the carotenoid content was about the same as in the respective control group (Figure 2B).

244 Chlorophyll *a* and carotenoids are important light-absorbing pigments and are essential for the process of
245 photosynthesis (Hirschberg and Chamovitz, 1994; Björn et al., 2009). Controversial findings have been
246 limiting the use of chlorophyll *a* and carotenoids as suitable biomass indicators (Caroppo et al., 2012; Sinetova
247 et al., 2012; Yu et al., 2023; Ramaraj et al., 2013; Prihantini et al., 2019). Therefore, chlorophyll *a* was here

248 used as a marker only for *H. metazoicum* viability and not for growth. The ability of *H. metazoicum* to face
249 different environmental conditions such as high temperature, irradiance and salinity has been already reported
250 (Mutalipassi et al., 2019a). Mattes of *H. metazoicum* that are in good conditions present a pigment profile with
251 chlorophyll *a* being the major photosynthetic pigment and with carotenoids in lower abundance as shown in
252 Figure 2A and 2B and in accordance with Caroppo et al. (2012), as seen in other cyanobacteria.
253 Here, results on the viability under acidified conditions suggest that *H. metazoicum* is able to tolerate low pH
254 conditions down to severe ones as 6.5, thus confirming what was expected from field observations with mattes
255 populating naturally acidified marine areas.

256 **3.3. Gene expression**

257 The ABC-like gene *slr2019* was found to be vital in *Synechocystis* sp. PCC6803 to tolerate acid stress
258 conditions (Matsuashi et al., 2015). Through the use of a *slr2019*-defective mutant strain, Matsuashi et al.
259 (2015) showed that *Synechocystis* sp. PCC6803 was not able to proliferate without this gene following
260 exposure to pH 6.0 of 7 d. Moreover, after a short-term (4 h) exposure to pH 3.0, *slr2019* gene expression was
261 found to be increased compared to a control, although the differences were not significant. Here, the *H.*
262 *metazoicum* *slr2019*-like gene was upregulated by 2.8 fold in mattes exposed to pH 7.7 for 7 d; this change
263 was not significant due to high variation across replicates, but upregulation was consistently seen in all
264 replicates of this treatment (Figure 2C). In contrast, a slight but not significant downregulation in *slr2019*
265 expression levels was observed in mattes from the pH-7.2 and pH-6.5 treatments (Figure 2C). On the opposite,
266 after 30 d of exposure, significant down-regulation of the *slr2019* gene was observed at all experimental pH
267 conditions compared to the control with fold changes in expression of 0.11 at pH 7.7, 0.03 at pH 7.2, and 0.04
268 at pH 6.5 (Figure 2C). Our results, at different pH and after 30-d exposure, provide additional information to
269 data of Matsuashi et al. (2015) indicating the response of cyanobacteria to acidified conditions, showing the
270 relationship between pH and its effects in gene regulation, and the importance of exposure of time. In order to
271 explain our findings two possible hypotheses were formulated.

272 Our first hypothesis would be that exposure of *H. metazoicum* to low pH causes changes in the membrane's-
273 lipopolysaccharide (LPS) structure as an acclimatation response to low-pH conditions. According to
274 McGowan et al. (1998) and Martinić et al. (2011), changes in bacterial LPS structure occur upon exposure to

275 low pH (5.0 - 5.5). *Synechocystis* sp. PCC6803's *Slr2019* is actually homologous to *Escherichia coli*'s inner
276 membrane ABC transporter MsbA (Matsuashi et al., 2015) which is responsible for the synthesis and
277 transportation of lipid A, one of the three major structures of LPS (Polissi and Georgopoulos, 1996; Zhou et
278 al., 1998). LPS represents the main component of the outer membrane in Gram-negative bacteria, including
279 cyanobacteria (Buttke and Ingram, 1975), and its synthesis and translocation is carried out by different
280 proteins, including several ABC transporters (Polissi and Georgopoulos, 1996; Zhou et al., 1998; Sperandeo
281 et al., 2007). LPS has a protective role for bacterial cells (Bertani and Ruiz, 2018) and previous findings have
282 shown its importance for the tolerance of bacteria to acid conditions (Martinić et al., 2011; McGowan et al.,
283 1998). In *Shigella flexneri* 2a, changes in the composition of two LPS regions, lipid A and O antigen, have
284 been observed upon overnight exposure to pH 5.5 (Martinić et al., 2011). McGowan et al. (1998) identified
285 the appearance of high-molecular-weight proteins and the down-regulated expression of other proteins in the
286 LPS profile of *Helicobacter pylori* following a 72-96-h exposure to pH 5.0. Thus, the alteration in LPS
287 structure seems to be due to an up-regulation of some LPS components and a down-regulation of other
288 elements. Matsuashi et al. (2015) have demonstrated that *Slr2019* is involved in LPS synthesis in *Synechocystis*
289 sp. PCC6803. Therefore, *Slr2019* of *H. metazoicum* may be involved in the synthesis and/or transport of a
290 LPS component which is more sensitive to moderate low-pH (7.7) in the short-term (7 d) and completely
291 abolished upon prolonged exposure (30 d).

292 Our second hypothesis would be that changes in *slr2019* gene expression could be ascribed to the decrease of
293 ATP caused by the increase of CO₂ intake which indeed has a strong effect on ATP pump transport
294 functionality. A rise in external *p*CO₂ causes an increase in CO₂ uptake by bacterial cells with consequences
295 for the intracellular ATP concentration. Physiological changes at higher CO₂ concentrations were reported by
296 Klangpetch et al. (2013) as a decrease in intracellular ATP concentration in *E. coli* exposed to *p*CO₂ of 1–6
297 MPa for 16 min. The reduction of ATP may indeed result in lower availability of energy for other cellular
298 pathways and may also impair ABC transporter activity. In order to compensate for lower ABC transporter
299 activity and to maintain their functionality, cells might enhance the transcription of *Slr2019*. Therefore, the
300 exposure to high-*p*CO₂ and the ATP depletion could be responsible for the observed up-regulation of the
301 *slr2019* gene in the short-term (after 7 d) at pH 7.7. The response pattern shown by *H. metazoicum* at lower

302 pH conditions (7.2, 6.5) and in a longer time (30 d) suggests that this initial up-regulation of *slr2019* is too
303 energetically too costly for cyanobacteria when exposed to more severe conditions.

304

305 **4. Conclusions**

306 This study represents a preliminary assessment of the modulation of ABC genes in *H. metazoicum* upon
307 exposure to low pH resembling future OA scenarios in agreement with previous findings in cyanobacteria and
308 other bacterial species, such as *Synechocystis* sp., through gene-deleted mutant strains and gene modulation
309 analysis (Tahara et al., 2012; 2015; Uchiyama et al., 2019).

310 The evolution of different RNA extraction methods enabled to identify a protocol that is suitable to break up
311 the cell walls of *H. metazoicum* so that RNA of high quality and quantity can be obtained. Such RNA could
312 be used for transcript-level analyses of the ABC-like gene *slr2019*.

313 *H. metazoicum* has been shown to tolerate low pH conditions down to 6.5, far lower than environmental future
314 predicted scenarios since pigment analyses indicated no adverse effects of acidified environments on
315 cyanobacterial viability. Slr2019 function could thus compensate for adverse effects of low pH after short term
316 exposure to environmental relevant value (7.7), this may be indicated by the up-regulation of *slr2019*. On the
317 other hand, downregulation of *slr2019* after 30 d with decreasing pH suggests that this is not the case and
318 further studies are needed to investigate whether this is associated with an adverse effect of low pH.

319 Since a different behaviour in *slr2019* gene expression was observed between 7 and 30 d, further investigations
320 are necessary to unravel the mechanism of specific involvement. Such knowledge will allow us to further
321 investigate the ability of marine species to deal with OA scenarios and predict future impacts on biodiversity.

322

323 **CRedit authorship contribution statement**

324 **Romano Patrizia:** Methodology, Formal analysis, Investigation, Data Curation, Writing - Original Draft,
325 Writing - Review & Editing. **Simonetti Silvia:** Conceptualization, Methodology, Formal analysis,
326 Investigation, Data Curation, Writing - Original Draft, Writing - Review & Editing, Visualization, Supervision.

327 **Maria Cristina Gambi:** Conceptualization, Methodology, Writing - Review & Editing, Supervision, Project

328 administration, Funding acquisition. **Till Luckenbach**: Writing - Review & Editing. **Valerio Zupo**:
329 Conceptualization, Methodology, Resources, Writing - Review & Editing, Supervision, Project administration,
330 Funding acquisition. **Iaria Corsi**: Conceptualization, Methodology, Resources, Writing - Review & Editing,
331 Supervision, Project administration, Funding acquisition.

332 **Declaration of competing interest**

333 The authors declare no competing interests.

334 **Acknowledgements**

335 The authors thank Tatiana Rusconi (PhD candidate at the University of Siena) for her help in image editing.
336 Thanks are due to Emanuele Somma (former PhD at the University of Trieste and Stazione Zoologica Anton
337 Dohrn) and Mirko Mutalipassi (former post-doc, Stazione Zoologica Anton Dohrn) for the help during *H.*
338 *metazoicum* exposition at the Ischia Marine Centre. Finally, the authors also acknowledge Maria Cristina
339 Fossi's Lab. (Department of Physical, Earth and Environmental Sciences, University of Siena, Italy), in
340 particular Dr. Cristina Panti and Dr. Giacomo Limonta, for their support with the real-time PCR instrument.

341 **Funding sources**

342 This work was supported by the 2020 scholarship co-founded by the University of Siena and the Stazione
343 Zoologica Anton Dohrn of Naples entitled 'Molecular bases and evolutionary constraints of cellular acid
344 tolerance in cyanobacteria and invertebrates subjected to ocean acidification and other sources of stress'
345 (METASTRESS) in the framework of the Doctoral Research Program in Environmental, Geological and Polar
346 Sciences and Technologies (36th cycle) of the University of Siena.

347 **5. References**

- 348 Alter, K., Jacquemont, J., Claudet, J., Lattuca, M.E., Barrantes, M.E., Marras, S., Manríquez, P.H.,
349 González, C.P., Fernández, D.A., Peck, M.A., Cattano, C., Milazzo, M., Mark, F.C., Domenici, P., 2024
350 Hidden impacts of ocean warming and acidification on biological responses of marine animals revealed
351 through meta-analysis. *Nat. Commun.* 15, 2885. <https://doi.org/10.1038/s41467-024-47064-3>.
- 352 Aranda, P.S., LaJoie, D.M., Jorcyk, C.L., 2012. Bleach gel: A simple agarose gel for analyzing RNA quality.
353 *Electrophoresis* 33 (2), 366–369. 10.1002/elps.201100335.
- 354 Bertani, B., Ruiz, N., 2018. Function and biogenesis of lipopolysaccharides. *EcoSal Plus* 8 (1),
355 10.1128/ecosalplus.ESP-0001-2018. 10.1128/ecosalplus.ESP-0001-2018.
- 356 Bindoff, N.L., Cheung, W.W.L., Kairo, J.G., Arístegui, J., Guinder, V.A., Hallberg, R., Hilmi, N., Jiao, N.,
357 Karim, M.S., Levin, L., O'Donoghue, S., Purca Cuicapusa, S.R., Rinkevich, B., Suga, T., Tagliabue, A.,
358 Williamson, P., 2019. Changing ocean, marine ecosystems, and dependent communities. In: Pörtner, H.-O.,
359 Roberts, D.C., Masson- Delmotte, V., Zhai, P., Tignor, M., Poloczanska, E., Mintenbeck, K., Alegría, A.,
360 Nicolai, M., Okem, A., Petzold, J., Rama, B., Weyer, N.M. (Eds.), *IPCC Special Report on the Ocean and*
361 *Cryosphere in a Changing Climate*. [Pörtner, H.-O., Roberts, D.C., Masson-Delmotte, V., Zhai, P., Tignor, M.,
362 Poloczanska, E., Mintenbeck, K., Alegría, A., Nicolai, M., Okem, A., Petzold, J., Rama, B., Weyer, N.M.
363 (eds.)]. Cambridge University Press, Cambridge, UK and New York, NY, USA, pp. 447-587.
364 10.1017/9781009157964.007.
- 365 Björn, L.O., Papageorgiou, G.C., Blankenship, R.E., Govindjee, 2009. A viewpoint: Why chlorophyll *a*?
366 *Photosynth. Res.* 99, 85 – 98. <https://doi.org/10.1007/s11120-008-9395-x>.
- 367 Buttke, T.M., Ingram, L.O., 1975 Comparison of lipopolysaccharides from *Agmenellum quadruplicatum* to
368 *Escherichia coli* and *Salmonella typhimurium* by using thin-layer chromatography. *J. Bacteriol.* 124 (3), 1566
369 – 1573.
- 370 Caroppo, C., Albertano, P., Bruno, L., Montinari, M., Rizzi, M., Vigliotta, G., Pagliara, P., 2012. Identification
371 and characterization of a new *Halomiconema* species (Cyanobacteria) isolated from the Mediterranean marine

372 sponge *Petrosia ficiformis* (Porifera). Fottea, Olomouc 12 (2), 315–326.
373 <https://dx.doi.org/10.5507/fot.2012.022>.

374 Defrancesco, C., Costaraoss, S., Monauni, C., Pellegrini, G., Pozzi, S., 2002. Un metodo sperimentale per il
375 conteggio delle cellule di *Microcystis aeruginosa*: dati preliminari. *Biologia Ambientale* 16 (1), 7–11.

376 Doney, S.C., Fabry V.J., Feely, R.A., Kleypas, J.A., 2009. Ocean acidification: the other CO₂ problem. *Ann.*
377 *Rev. Mar. Sci.* 1, 169–192. [10.1146/annurev.marine.010908.163834](https://doi.org/10.1146/annurev.marine.010908.163834).

378 Fanelli, E., Di Giacomo, S., Gambi, C., Bianchelli, S., Da Ros, Z., Tangherlini, M., Andaloro, F., Romeo, T.,
379 Corinaldesi, C., Danovaro, R., 2022. Effects of local acidification on benthic communities at shallow
380 hydrothermal vents of the Aeolian Islands (Southern Tyrrhenian, Mediterranean Sea). *Biology* 11, 321.
381 <https://doi.org/10.3390/biology11020321>

382 Foo, S.A., Byrne, M. Gambi, M.C., Ricevuto, E., 2018. The carbon dioxide vents of Ischia, Italy, a natural
383 laboratory to assess impacts of ocean acidification on marine ecosystems: an overview of research and
384 comparisons with other vent systems. *Oceanogr. Mar. Biol. Annu. Rev.* 56, 237–310.

385 Gambi, M.C., Musco, L., Giangrande, A., Badalamenti, F., Micheli, F., Kroeker, K.J., 2016. Distribution and
386 functional traits of polychaetes in a CO₂ vent system: winners and losers among closely related species. *Mar.*
387 *Ecol. Prog. Ser.* 550, 121–134. <https://doi.org/10.3354/meps1172>.

388 Gao, L., Shi, W., Xia, X., 2023. Genomic plasticity of acid-tolerant phenotypic evolution in *Acetobacter*
389 *pasteurianus*. *Appl. Biochem. Biotechnol.* 195, 6003 – 6019. <https://doi.org/10.1007/s12010-023-04353-9>.

390 Hirschberg, J., Chamovitz, D., 1994. Carotenoids in Cyanobacteria. In: Bryant, D.A. (eds) *The molecular*
391 *biology of Cyanobacteria. Advances in photosynthesis, vol 1.* Springer, Dordrecht. [10.1007/978-94-011-0227-](https://doi.org/10.1007/978-94-011-0227-8_18)
392 [8_18](https://doi.org/10.1007/978-94-011-0227-8_18).

393 Jiang, L.-Q., Carter, B.R., Feely, R.A., Lauvset, S.K., Olsen, A., 2019. Surface ocean pH and buffer capacity:
394 past, present and future. *Sci. Rep.* 9, 18624. <https://doi.org/10.1038/s41598-019-55039-4>.

395 Kim Tiam, S., Comte, K., Dalle, C., Duval, C., Pancrace, C., Gugger, M., Marie, B., Yéprémian, C., Bernard,
396 C., 2019. Development of a new extraction method based on high-intensity ultra-sonication to study RNA

397 regulation of the filamentous cyanobacteria *Planktothrix*. PLoS ONE 14 (9), e0222029.
398 <https://doi.org/10.1371/journal.pone.0222029>.

399 Klangpetch, W., Noma, S., Igura, N., Shimoda, M., 2013. Effects of high-pressure carbonation on intracellular
400 ATP and NADH levels and DNA damage in *Escherichia coli* cells. Biocontrol Sci. 18 (4), 199–203.
401 [10.4265/bio.18.199](https://doi.org/10.4265/bio.18.199).

402 Kroeker, K.J., Micheli, F., Gambi, M.C., Martz, T.R. 2011. Divergent ecosystem responses within a benthic
403 marine community to ocean acidification. Proceedings of the National Academy of Sciences USA (PNAS),
404 108 (35), 14515–14520. DOI [10.1073/pnas.1107789108](https://doi.org/10.1073/pnas.1107789108).

405 Kroeker, K.J., Gambi, M.C., Micheli, F., 2013. Community dynamics and ecosystem simplification in a high-
406 CO₂ ocean. Proc. Natl. Acad. Sci. U. S. A. 110 (31), 12721–12726. <https://doi.org/10.1073/pnas.1216464110>.

407 Livak, K.J., Schmittgen, T.D., 2001. Analysis of relative gene expression data using Real-time quantitative
408 PCR and the $2^{-\Delta\Delta CT}$ Method. Methods 25, 402–408. [10.1006/meth.2001.1262](https://doi.org/10.1006/meth.2001.1262).

409 Martinić, M., Hoare, A., Contreras, I. and Álvarez, S. A., 2011. Contribution of the lipopolysaccharide to
410 resistance of *Shigella flexneri* 2a to extreme acidity. PLoS ONE, 6 (10), e25557. Doi:
411 [10.1371/journal.pone.0025557](https://doi.org/10.1371/journal.pone.0025557).

412 Matsushashi, A., Tahara, H., Ito, Y., Uchiyama, J., Ogawa, S., Ohta, H., 2015. Slr2019, lipid A transporter
413 homolog, is essential for acidic tolerance in *Synechocystis* sp. PCC6803. Photosynth. Res. 125 (1), 267–277.
414 [10.1007/s11120-015-0129-6](https://doi.org/10.1007/s11120-015-0129-6).

415 McGowan, C.C., Necheva, A., Thompson, S.A., Cover, T.L., Blaser, M.J., 1998. Acid-induced expression of
416 an LPS-associated gene in *Helicobacter pylori*. Mol. Microbiol. 30 (1), 19–31. [10.1046/j.1365-2958.1998.t01-1-01079.x](https://doi.org/10.1046/j.1365-2958.1998.t01-1-01079.x).

418 Munari, M., Chiarore, A., Signorini, S. G., Cannavacciuolo, A., Nannini, M., Magni, S., Binelli, A., Gambi,
419 M.C., Della Torre, C., 2022 Surviving in a changing ocean. Tolerance to acidification might affect the
420 susceptibility of polychaetes to chemical contamination. Mar. Pollut. Bull. 181, 113857.
421 <https://doi.org/10.1016/j.marpolbul.2022.113857>.

422 Muralisankar, T., Kalaivania, P., Thangala, S.H., Santhanam, P., 2021. Growth, biochemical, antioxidants,
423 metabolic enzymes and hemocytes population of the shrimp *Litopenaeus vannamei* exposed to acidified
424 seawater. *Comp. Biochem. Physiol.* 239 (C), 108843. <https://doi.org/10.1016/j.cbpc.2020.108843>.

425 Mutalipassi, M., Mazzella, V., Romano, G., Ruocco, N., Costantini, M., Glaviano, F., Zupo, V., 2019a. Growth
426 and toxicity of *Halomicronema metazoicum* (Cyanoprokaryota, Cyanophyta) at different conditions of light,
427 salinity and temperature. *Biol. Open.* 8, bio043604. 10.1242/bio.043604.

428 Mutalipassi, M., Mazzella, V., Zupo, V., 2019b. Ocean acidification influences plant-animal interactions: the
429 effect of *Cocconeis scutellum parva* on the sex reversal of *Hippolyte inermis*. *PLoS One* 14, e0218238.
430 <https://doi.org/10.1371/journal.pone.0218238>.

431 Nakano, S., Fukaya, M., Horinouchi, S., 2006. Putative ABC transporter responsible for acetic acid resistance
432 in *Acetobacter aceti*. *AEM* 72 (1), 497–505. 10.1128/AEM.72.1.497-505.2006.

433 Polissi, A., Georgopoulos, C., 1996. Mutational analysis and properties of the *msbA* gene of *Escherichia coli*,
434 coding for an essential ABC family transporter. *Mol. Microbiol.* 20 (6), 1221–1233. 10.1111/j.1365-
435 2958.1996.tb02642.x.

436 Prihantini, N.B., Pertiwi, Z.D., Yuniati, R., Sjamsuridzal, W., Putrika, A., 2019. The effect of temperature
437 variation on the growth of *Leptolyngbya* (cyanobacteria) HS-16 and HS-36 to biomass weight in BG-11
438 medium. *Biocatal. Agric. Biotechnol.* 19, 101105. <https://doi.org/10.1016/j.bcab.2019.101105>.

439 Ramaraj, R., Tsai, D.D.-W., Chen, P.H., 2012. Chlorophyll is not accurate measurement for algal biomass.
440 *Chiang Mai J. Sci.* 40 (4), 547–555.

441 Ruocco, N., Mutalipassi, M., Pollio, A., Costantini, S., Costantini, M., Zupo, V., 2018. First evidence of
442 *Halomicronema metazoicum* (Cyanobacteria) free-living on *Posidonia oceanica* leaves. *PloS One* 13 (10),
443 e0204954. <https://doi.org/10.1371/journal.pone.0204954>.

444 Shvarev, D., Maldener, I., 2020. The HlyD-like membrane fusion protein All5304 is essential for acid stress
445 survival of the filamentous cyanobacterium *Anabaena* sp. PCC 7120. *FEMS Microbiol. Lett.* 367 (15).
446 <https://doi.org/10.1093/femsle/fnaa108>.

447 Simonetti, S., Zupo, V., Gambi, M.C., Luckenbach, T., Corsi, I., 2022 Unraveling cellular and molecular
448 mechanisms of acid stress tolerance and resistance in marine species: New frontiers in the study of adaptation
449 to ocean acidification. *Mar. Pollut. Bull.* 185, 114365. <https://doi.org/10.1016/j.marpolbul.2022.114365>.

450 Sinetova, M.A., Červený, J., Zavřel, T., Nedbal, L., 2012. On the dynamics and constraints of batch culture
451 growth of the cyanobacterium *Cyanothece* sp. ATCC 51142. *J. Biotechnol.* 162, 148–155.
452 <http://dx.doi.org/10.1016/j.jbiotec.2012.04.009>.

453 Sperandeo, P., Cescutti, R., Villa, R., Di Benedetto, C., Candia, D., Dehò, G., Polissi, A. 2007 Characterization
454 of *lptA* and *lptB*, two essential genes implicated in lipopolysaccharide transport to the outer membrane of
455 *Escherichia coli*. *J. Bacteriol.* 189 (1), 244–253. 10.1128/JB.01126-06.

456 Tahara, H., Uchiyama, J., Yoshihara, T., Matsumoto, K., Ohta, H., 2012. Role of Slr1045 in environmental
457 stress tolerance and lipid transport in the cyanobacterium *Synechocystis* sp. PCC6803. *Biochim. Biophys. Acta*
458 1817, 1360–1366. 10.1016/j.bbabbio.2012.02.035.

459 Tahara, H., Matsushashi, A., Uchiyama, J., Ogawa, S., Ohta, H., 2015. Sll0751 and Sll1041 are involved in acid
460 stress tolerance in *Synechocystis* sp. PCC 6803. *Photosynth. Res.* 125, 233–242.
461 <https://doi.org/10.1007/s11120-015-0153-6>.

462 Teixidó, N., Gambi, M.C., Parravacini, V., Kroeker, K., Micheli, F., Villéger, S., Ballesteros, E., 2018.
463 Functional biodiversity loss along natural CO₂ gradients. *Nat. Commun.* 9, 5149.
464 <https://doi.org/10.1038/s41467-018-07592-1>.

465 Uchiyama, J., Itagaki, A., Ishikawa, H., Tanaka, Y., Kohga, H., Nakahara, A., Imaida, A., Tahara, H., Ohta,
466 H., 2019. Characterization of ABC transporter genes, *sll1180*, *sll1181*, and *slr1270*, involved in acid stress
467 tolerance of *Synechocystis* sp. PCC 6803. *Photosynth. Res.* 139, 325–335. [https://doi.org/10.1007/s11120-018-](https://doi.org/10.1007/s11120-018-0548-2)
468 0548-2.

469 Vizzini, S., Martínez-Crego, B., Andolina, C., Massa-Gallucci, A., Connell, S.D., Gambi, M.C., 2017. Ocean
470 acidification as a driver of community simplification via the collapse of higher-order and rise of lower-order
471 consumers. *Sci. Rep.* 7, 4018. <http://10.0.4.14/s41598-017-03802-w>.

472 Wang, L., Stegemann, J.P., 2010. Extraction of high quality RNA from polysaccharide matrices using
473 cetyltrimethylammonium bromide. *Biomater.* 31 (7), 1612–1618. [10.1016/j.biomaterials.2009.11.024](https://doi.org/10.1016/j.biomaterials.2009.11.024).

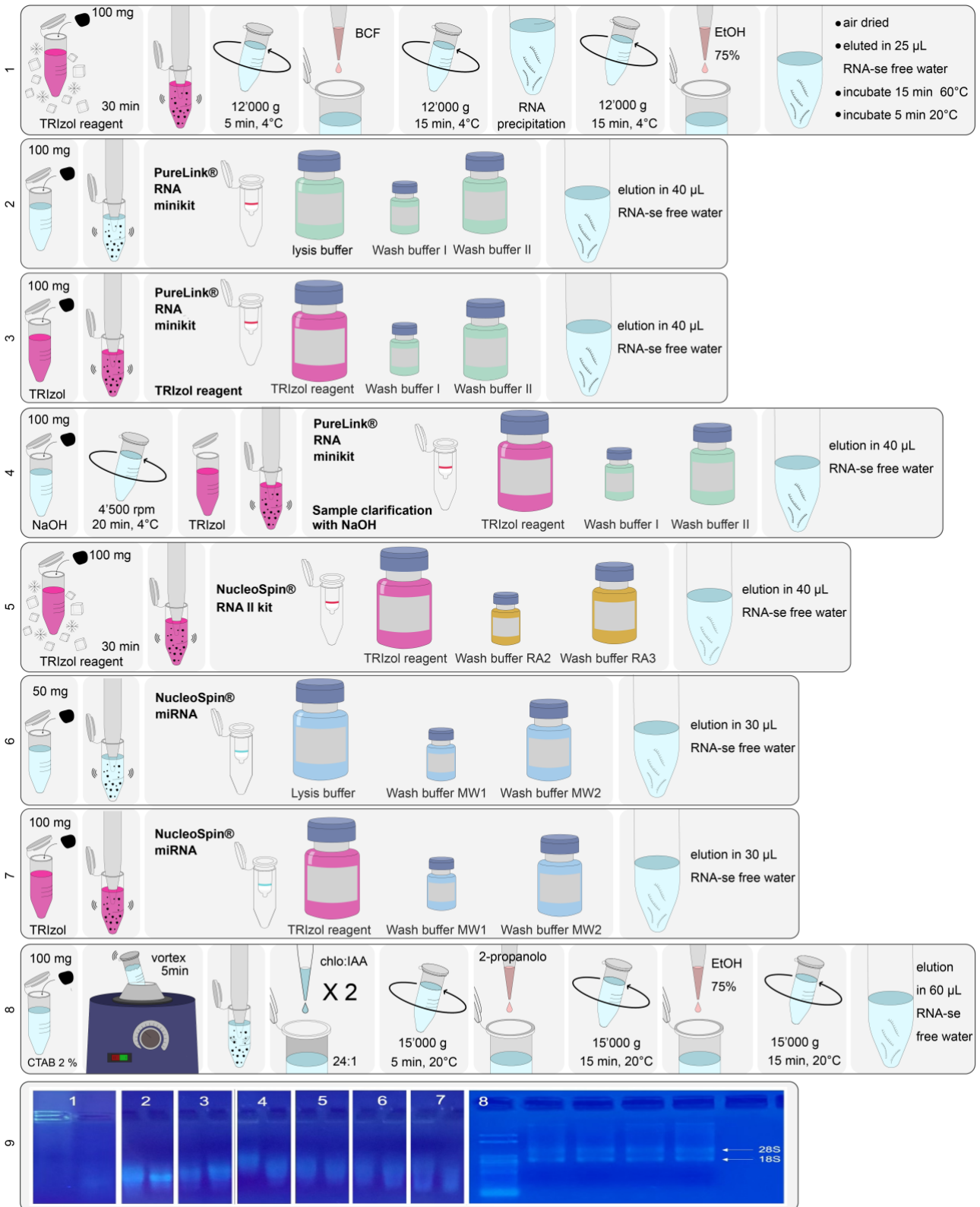
474 Xie, J., Sun, X., Li, P., Zhou, T., Jiang, R., Wang, X., 2023. The impact of ocean acidification on the eye,
475 cuttlebone and behaviors of juvenile cuttlefish (*Sepiella inermis*). *Mar. Pollut. Bull.* 190, 114831.
476 <https://doi.org/10.1016/j.marpolbul.2023.114831>.

477 Yu, J., Zhu, H., Wang, H., Shutes, B., Niu, T., 2023. Effect of butachlor on *Microcystis aeruginosa*: Cellular
478 and molecular mechanisms of toxicity. *J. Hazard. Mater.* 449, 131042.
479 <https://doi.org/10.1016/j.jhazmat.2023.131042>.

480 Zavřel, T., Sinetova, M.A., Červený, J., 2015. Measurement of chlorophyll *a* and carotenoids concentration in
481 Cyanobacteria. *Bio-protoc.* 5 (9), e1467. [10.21769/BioProtoc.1467](https://doi.org/10.21769/BioProtoc.1467).

482 Zhou, Z., White, K. A., Polissi, A., Georgopoulos, C., Raetz, C.R.H., 1998. Function of *Escherichia coli*
483 MsbA, an essential ABC family transporter, in lipid A and phospholipid biosynthesis. *JBC* 273 (20), 12466–
484 12475. <https://doi.org/10.1074/jbc.273.20.12466>.

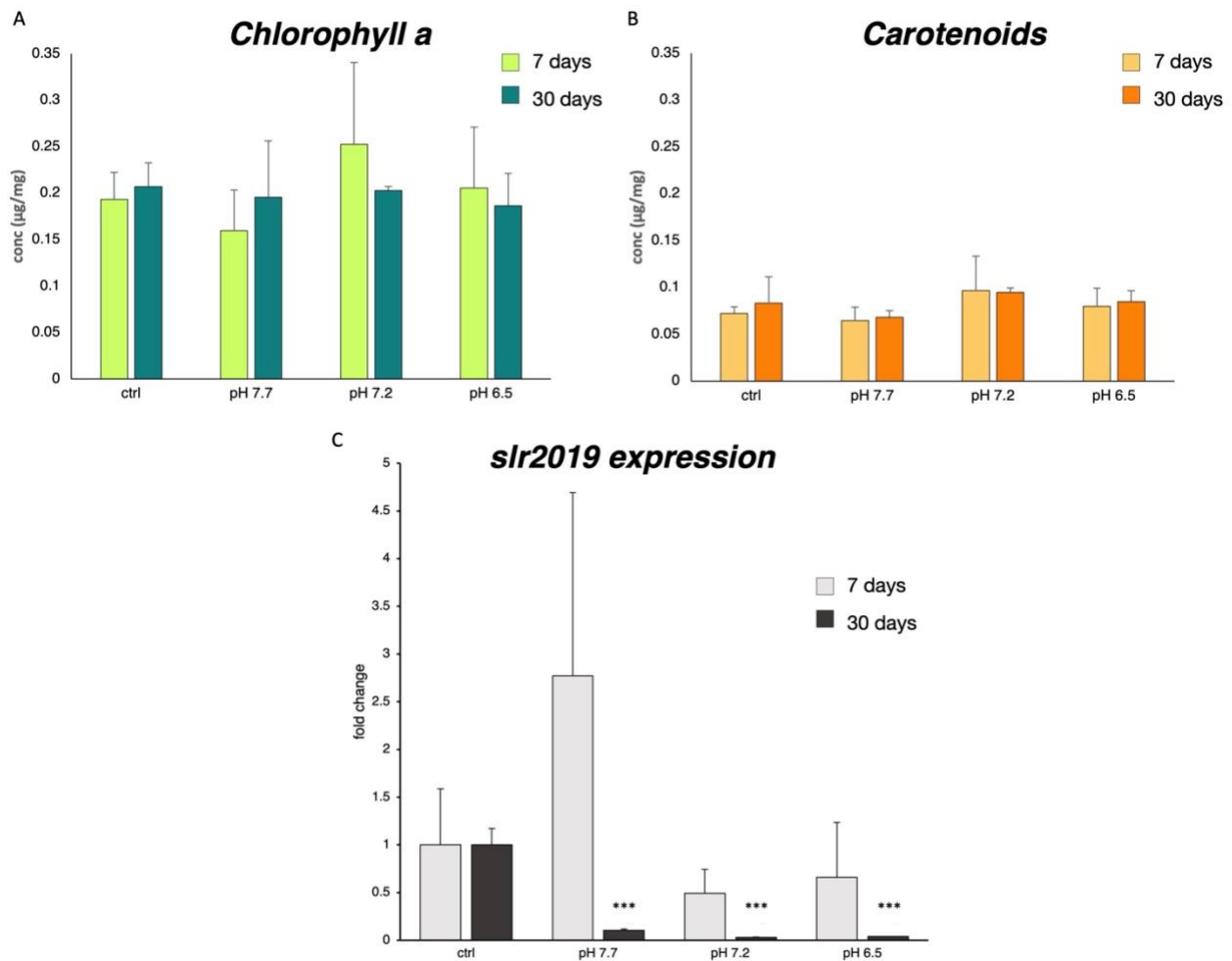
485 Zhu, Z., Yang, Y., Yang, P., Wu, Z., Zhang, J., Du, G., 2019. Enhanced acid-stress tolerance in *Lactococcus*
486 *lactis* NZ9000 by overexpression of ABC transporters. *Microb. Cell. Factories.* 18, 136.
487 <https://doi.org/10.1186/s12934-019-1188-8>.



488

489 Figure 1. Schematic description of the extraction methods (1-8) and 1.5% agarose 'bleach gel' showing the quality of the
 490 extracted RNA from each method (9). White arrows indicate 18S and 28S ribosomal RNA bands

491 2-column fitting image, color online only



492

493 Figure 2. Physiological and transcriptomic results assessed in *H. metazoicum* mattes exposed to four different pH (8.2,
 494 7.7, 7.2, 6.5). The upper charts represent chlorophyll *a* (A) and carotenoid (B) contents (µg/mg) measured in control and
 495 treated groups after 7 and 30 d of exposure. The chart below (C) represents the expression of *slr2019* gene in control and
 496 treated groups after 7 and 30 d of exposure. Results are shown as mean ± standard deviation (SD). *** indicates significant
 497 differences ($p < 0.001$) with controls group

498 2-column fitting image, color online only

499 Table 1. Table of purity, concentrations and yield (mean \pm standard deviation) of total RNA extracted through the eight
 500 different methods

	$A_{260/280}$	$A_{260/230}$	Conc (ng _{RNA} /μL)	Yield (ng _{RNA} /mg _{sample})
Manual extraction	1.86 \pm 0.14	0.10 \pm 0.00	105.97 \pm 29.77	12.89 \pm 3.78
PureLink® RNA Mini Kit	1.80 \pm 0.03	0.61 \pm 0.07	74.70 \pm 18.24	14.88 \pm 3.73
TRIzol + PureLink	1.99 \pm 0.07	1.23 \pm 0.44	23.67 \pm 29.57	4.63 \pm 5.68
NaOH + PureLink	1.94 \pm 0.07	0.63 \pm 0.31	8.05 \pm 3.05	1.13 \pm 0.14
NucleoSpin® RNA II Kit	1.57 \pm 0.38	0.42 \pm 0.48	33.65 \pm 5.59	6.72 \pm 1.47
NucleoSpin® miRNA Kit	2.10 \pm 0.02	1.52 \pm 0.03	9.60 \pm 0.42	5.97 \pm 0.26
TRIzol + NucleoSpin® miRNA Kit	2.01 \pm 0.08	1.24 \pm 0.33	7.15 \pm 3.08	2.91 \pm 1.30
CTAB 2% buffer	2.13 \pm 0.02	2.05 \pm 0.15	24.82 \pm 4.06	14.88 \pm 2.43

501